

CHAPTER 4

REACTOR STATICS

The study of a nuclear reactor operating in a steady-state is termed reactor statics; both short and long time variations represent dynamic characteristics and will be discussed in the next chapters. Our description here will focus on certain reactor core parameters such as neutron multiplication and on some basic spatial distributions such as the neutron flux.

4.1 REACTOR CRITICALITY

We begin our analysis of the reactor core with a description of the neutron induced fission process. In Fig. 4.1 we show graphically some of the events which lead to the steady-state condition in a CANDU nuclear reactor. A slow or thermal neutron, possessing a speed of approximately 2200 m/s, is absorbed in a Uranium-235 nucleus. This Uranium-236 nucleus subsequently breaks up into two fission fragments of unequal mass and concurrently emits several high energy neutrons whose energies are in the MeV range. These high energy neutrons subsequently migrate through the reactor core and, in doing so, may undergo a number of reactions; for example, they may become absorbed in the structural material in the core or even escape from the reactor core entirely. The one process of particular importance to the CANDU reactor is that the neutron loses its large kinetic energy by elastic collision predominantly in the heavy water moderator. Once the neutron has attained a relative low kinetic energy it is more likely to induce fission in Uranium-235 and thus contribute to the maintenance of the chain reaction. Such a sequence of events represents a life-history of a neutron and may be viewed as one generation. The time required for this cycle is relatively short, about 0.001 s; the path traced out by a neutron during its life-history may very well exceed several meters.

Several pertinent questions come to mind when considering the above sequence of events. How is it possible to insure that for every one neutron which causes fission exactly one neutron will cause a subsequent fission in order that a steady-state chain reaction can be maintained? How is the chain reaction influenced by the material composition of the core and by the size of the reactor? What is the role of the neutron density and what is the effect of fission products? Some of the answers to these questions will become clear forthwith while others will be discussed in subsequent chapters.

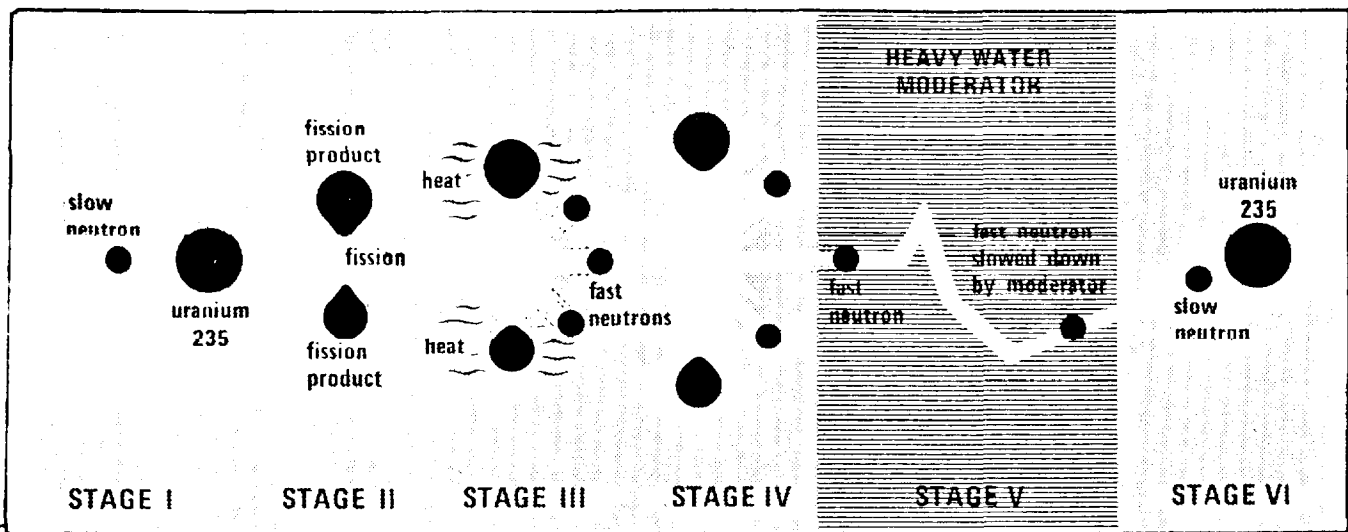


FIG. 4.1: Illustration of fission chain reaction and subsequent events.

One parameter which has become widely used in the analysis of nuclear reactors is called the effective multiplication constant and identified by the symbol k_{eff} . This parameter represents the ratio of neutrons of two successive generations in a finite reactor. That is

$$k_{eff} = \frac{\text{Number of neutrons in a subsequent generation}}{\text{Number of neutrons in the preceding generation}} \quad (4.1)$$

Clearly, if $k_{eff} = 1$, a steady-state condition exists because the neutron population does not change with time. If $k_{eff} > 1$ then the neutron density is increasing with time and, since the reactor power varies with the number of neutrons causing fission, the reactor power increases with time; such a situation exists during reactor start-up. If $k_{eff} < 1$ then the fission rate decreases with time since the neutron density decreases. These effects are graphically illustrated in Fig. 4.2.

The above description suggests an effective method of reactor control: it is a matter of controlling the number of neutrons in the reactor. If the reactor power is to be decreased or if the reactor is to be shut down, then control rods containing strong neutron absorbing materials are inserted into the core; the neutrons absorbed in the control rod thus contribute to a neutron deficiency in the core resulting in a decrease in the fission rate. Withdrawal of the control rods has the reverse effect. Other possibilities such as neutron booster rods and moderator level variation may also be employed in reactor control and will be discussed in subsequent chapters.

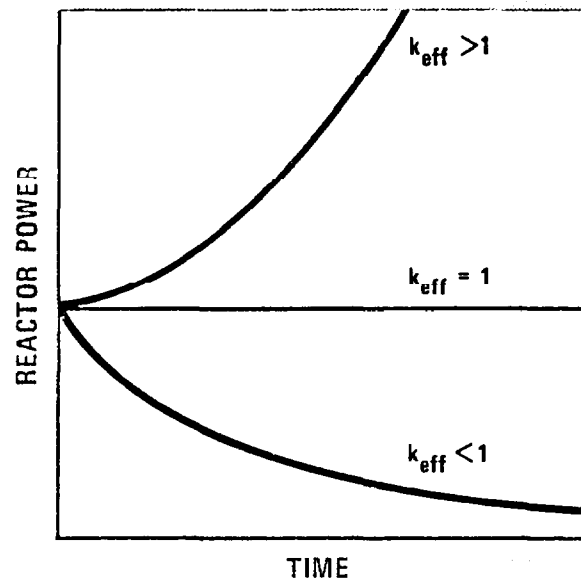


FIG. 4.2: Variation of reactor power with time for different values of the effective multiplication constant k_{eff} .

We now consider some of the reaction processes which effect the number of neutrons in successive generation to permit a quantitative representation for k_{eff} . The numerical values chosen here for the various parameters will be those which approximately apply to the CANDU reactor.

1. Initial Condition

We suppose that initially 100 neutrons appear in a given neutron generation as a result of the fission processes. That is, the denominator in Eq. (4.1) is 100; we now wish to follow these 100 neutrons through a complete cycle and thus determine the expression for the numerator in Eq. (4.1).

2. Fast Fission

Before these 100 neutrons have a chance to slow down, several of these high energy neutrons, say 2, may cause fission in two Uranium-238 nuclei; supposing that in one fission we have 3 fission neutrons appearing while in the other 2. Thus, the number of neutrons has increased to 103. This effect is called the fast fission effect and is described by the fast fission factor, ϵ , which, in this case, has the value

$$\epsilon = \frac{(100 - 2) + 5}{100} = 1.03 \quad (4.2)$$

3. Fast Neutron Leakage

Since these 103 neutrons possess a relatively high energy their

path between interactions with nuclei is very large. Hence, some of these neutrons may escape entirely from the reactor core. Supposing that 4 neutrons escape; this now leaves $103 - 4 = 99$ neutrons of the original 100. This effect is called the fast non-leakage probability, P_F , and is given by

$$P_F = \frac{103 - 4}{103} = 0.961 . \quad (4.3)$$

4. Resonance Escape Probability

The remaining 99 neutrons now undergo a slowing down process involving primarily elastic scattering in the moderator. However, in the course of neutron migration, some of these neutrons may encounter isotopes such as Uranium-238 which exhibits very strong resonance absorption in the intermediate energy range. Some 10% of the fission neutrons are absorbed in these resonances leaving $99 - 10 = 89$ neutrons. This possibility serves to define the resonance escape probability, p , which in this case, has the value of

$$p = \frac{99 - 10}{99} = 0.899 . \quad (4.4)$$

5. Thermal Utilization

Now that 89 of the original 100 neutrons have reached thermal energy we must recognize that neutron absorption can take place in materials other than in the nuclear fuel. Approximately 5 neutrons are removed in this parasitic process leaving $89 - 5 = 84$ neutrons. The factor describing this phenomena, designated by, f , and called thermal utilization, is therefore given by

$$f = \frac{89 - 5}{84} = 0.944 . \quad (4.5)$$

6. Thermal Neutron Leakage

In a manner similar to fast neutron leakage, thermal neutrons may also leak from the reactor core as well. This may involve some 4 neutrons leaving $84 - 4 = 80$ neutrons. The appropriate thermal non-leakage probability, P_T , is found to be

$$P_T = \frac{84 - 4}{84} = 0.952 . \quad (4.6)$$

7. Fission Neutrons per Neutrons Absorbed

Having following the history of 100 neutrons through the various events we have now arrived at the point where of the original 100 neutrons 80 are now absorbed in natural uranium. Not all of these lead to fission because uranium does have a definite parasitic capture cross section. However, the ratio of fission neutrons emitted per thermal neutron absorbed is of the order 1.25; this parameter is represented by the symbol η :

$$\eta = 1.25 . \quad (4.7)$$

Hence, the number of new fission neutrons resulting from the absorption of the 80 thermal neutrons is therefore

$$\eta \times 80 = 1.25 \times 80 = 100 . \quad (4.8)$$

Thus starting with an initial set of 100 fast fission neutrons, the same number of neutrons has been produced in the subsequent generation.

The definition for k_{eff} may now be cast in quantitative form. Retracing our steps above we note that the number of neutrons in the second generation is given by the product of the factors enumerated: $100\epsilon P_F P_T \eta$. The effective multiplication constant is hence represented by

$$k_{eff} = \frac{100\epsilon p f \eta P_F P_T}{100} = \epsilon p f \eta P_F P_T , \quad (4.9)$$

where the factor 100 has been cancelled in the numerator and denominator. That is, k_{eff} is independent of the number of initial neutrons and hence is not effected by power level.

The first four factors in Eq. (4.9) - often called the four-factor-formula - is the multiplication constant appropriate for a reactor of infinite size and represented by

$$k_{\infty} = \epsilon p f \eta . \quad (4.10)$$

The product $P_F P_T$ accounts for fast and thermal leakage associated with reactors of finite size. We may therefore write

$$k_{eff} = k_{\infty} P , \quad (4.11)$$

where P represents the probability that neither a slow nor a fast neutron will escape from the reactor.

The neutron cycle, as discussed above, is illustrated graphically in Fig. 4.3.

4.2 APPROACH TO CRITICAL

In the preceding section we described the several processes which are of particular importance to the determination of the state of criticality of a fissile assembly. Each parameter listed in Eq. (4.9) can, in principle, be calculated for a given material composition possessing a specified geometric shape. Indeed, these calculations are always carried out to determine the fuel loading of a nuclear reactor. This is not to suggest that, based on calculations alone, the reactor core materials are assembled up to the composition specified and that it is then expected to be exactly critical. Indeed, because of uncertainties

in the nuclear processes involved and approximations in the mathematical and calculational models, it is required practice that an approach to critical procedure be employed when the reactor is first made critical.

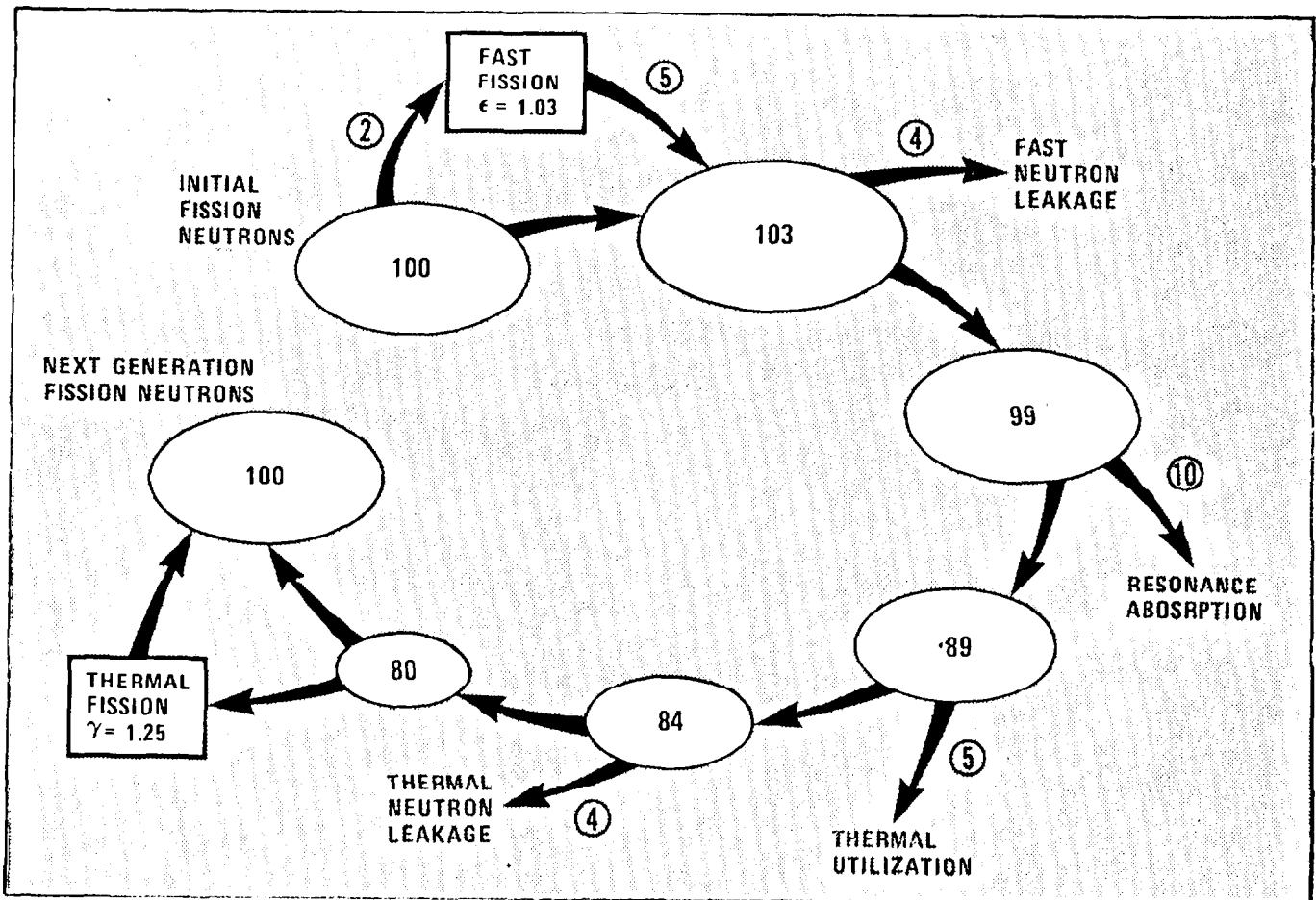


FIG. 4.3: Illustration of the neutron cycle; the numerical values listed are approximate and correspond to the values used in the text.

The approach to critical can best be described by reference to a graphical representation. Consider Stage I of Fig. 4.4. This represents the reactor core fully loaded with fuel but containing no moderator. Since any fission neutrons which might thus appear - either as a result of spontaneous fission or induced by a small isotopic neutron source - will not slow down due to the absence of a moderator, very few thermal neutrons which might cause fission will exist, hence the reactor is far subcritical.

Now consider the case in which some heavy water moderator has been added, Stage II in Fig. 4.4. Some neutron moderation is now taking place and, as a consequence, some neutron multiplication is occurring. As more moderator is added, more

fissions occur and the neutron density in the core increases to a new level. Eventually, at some critical height of the moderator, criticality will occur which means that a strict balance exists between (1) neutron production by fission, (2) neutron removal by absorption, and (3) neutron escape from the reactor by leakage. From here on, the appropriate management of control rods provides the necessary operating mechanism.

The above can be described analytically and thus provide a basis for monitoring the approach to critical. Supposing a neutron detector were located so as to provide an indication of an average neutron density in the moderator. If, at a given time during the approach to critical, the effective multiplication constant was given by k_{eff} then if n number of neutrons are introduced in the reactor core they will produce nk_{eff} neutrons in the second generation. These nk_{eff} neutrons subsequently lead to $(nk_{eff})k_{eff} = nk_{eff}^2$ neutrons in the next generation and so on. The neutron density as recorded by the detector at any moderator level is given by the infinite series

$$\begin{aligned} S &= n + nk_{eff} + nk_{eff}^2 + nk_{eff}^3 + \dots, \\ &= n(1 + k_{eff} + k_{eff}^2 + k_{eff}^3 + \dots). \end{aligned} \quad (4.12)$$

Since the reactor is subcritical, k_{eff} is less than unity and the above series can be shown to be written as

$$S = n\left(\frac{1}{1 - k_{eff}}\right). \quad (4.13)$$

As the moderator level continued to be raised, k_{eff} approaches unity and hence the neutron count rate, S , approaches an increasingly large number. The moderator height at which the reactor is critical is determined by extrapolation the

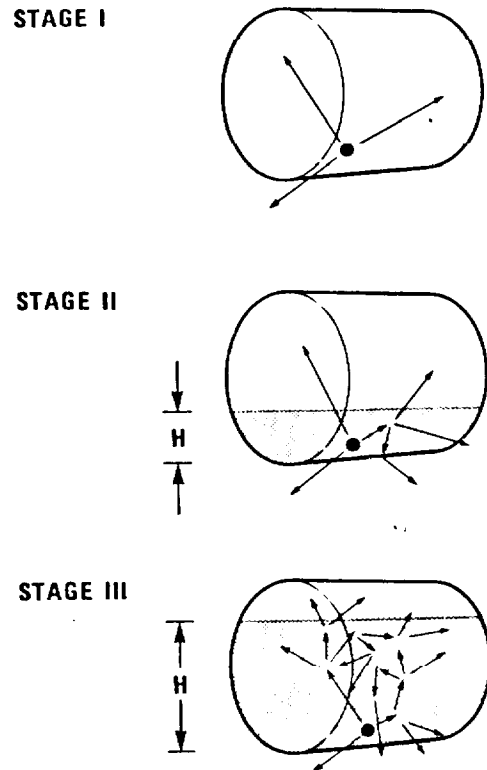


FIG. 4.4: Illustration of the approach to critical. The moderator level is successively raised and the neutron density measured at each step.

the inverse of the detector count rate, $1/S$, to zero. This is graphically shown in Fig. 4.5. Except for emergency dumps and other designed operating procedures, the moderator level is kept just below this critical height. The control rods are then used to provide overall reactor control. This subject will be further discussed in a subsequent chapter. Of more immediate interest in the problem of specifying the neutron flux in the reactor core.

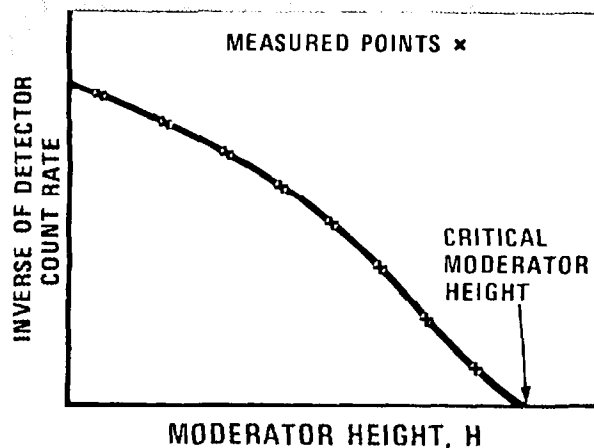


FIG. 4.5: Inverse of neutron detector count rate as a function of moderator height.

4.3 NEUTRON DIFFUSION ANALYSIS

In the preceding sections we have discussed some of the processes which are important to the attainment of a steady-state critical condition in a reactor core. We now consider such a steady-state core from the standpoint of determining the neutron density or the neutron flux density. A knowledge of how the flux varies in a reactor is important since many of the vital processes, such as fuel burnup, are directly related to the neutron flux.

We recall that the neutron-nucleus interaction density at a point \underline{r} in the core for the i 'th type of process may be written

$$F_i(\underline{r}) = \sigma_i N n(\underline{r}) v = \Sigma_i \phi(\underline{r}), \quad (4.14)$$

where the symbolism is used as defined previously. Also, in view of our discussion of energy dependence, we assume here that the neutron flux, $\phi(\underline{r})$ is suitably averaged so that Eq. (4.14) adequately represents the interaction density rate (neutrons/cm³-s) at the point \underline{r} . The above expression may be termed an energy-averaged interaction density.

When listing the fission density rate and neutron absorption density rate, Chapter 3, we noted that the neutron flux $\phi(\underline{r})$ represents a factor in each of these representations. Indeed, the neutron flux can be considered to be the most widely used distribution function in the analysis of a nuclear reactor core. The dimensions of this quantity is neutrons/cm²-s and suggests the totality of neutrons which pass through a unit area in all directions during one second. Another interpretation is to visualize the neutron flux as the total path of all neutrons in a unit volume formed per second. Fig. 4.6 provides a graphical representation of the flux $\phi(\underline{r})$ and also shows a graphical representation of the neutron density $n(\underline{r})$.

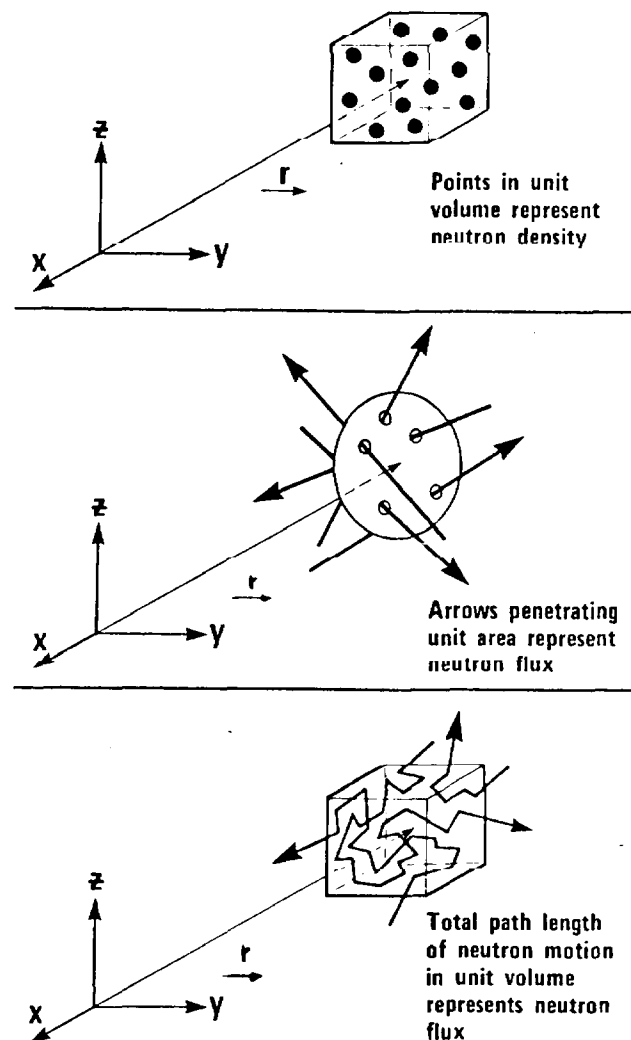


FIG. 4.6: Graphical representation of the neutron density and neutron flux.

The determination of the flux in our simplified reactor follows from a consideration of neutron conservation for an arbitrary differential volume element and a subsequent solution of a differential equation. Consider an arbitrary volume element about the vector point \underline{r} in the reactor core, Fig. 4.7. In order to maintain a steady-state condition, we must have a strict equality between the number of neutrons produced as a result of the fission process and the number of neutrons absorbed and leaked from the volume element:

$$\left(\begin{array}{l} \text{Number of neutrons} \\ \text{produced by fission} \\ \text{in volume element } dV \end{array} \right) = \left(\begin{array}{l} \text{Number of neutrons} \\ \text{absorbed in volume} \\ \text{element } dV \end{array} \right) + \left(\begin{array}{l} \text{Number of neutrons} \\ \text{leaking from volume} \\ \text{element } dV \end{array} \right) \quad (4.15)$$

In view of our discussion in Chapter 3, Section 4, we know that the neutron absorption rate per unit volume is given by

$$\text{Neutron absorption rate} = \Sigma_a \phi(\underline{r}) . \quad (4.16)$$

The number of neutrons produced by fission as a result of neutron absorption is equal to the absorption rate times the neutron multiplication constant k_{∞} . Hence,

$$\text{Neutron production rate} = k_{\infty} \Sigma_a \phi(\vec{r}) \quad , \quad (4.17)$$

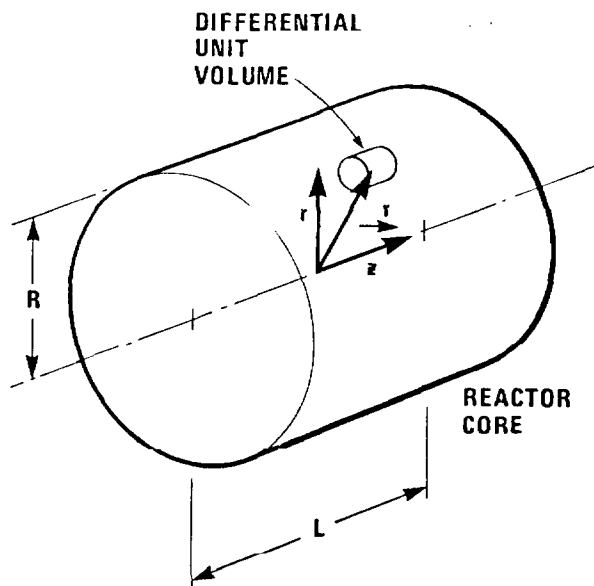


FIG. 4.7: Differential arbitrary volume element in reactor core.

The neutron leakage term in Eq. (4.15) can be determined from a detailed neutron conservation analysis. We consider the following procedure. Let $\vec{j}(\vec{r})$ represent the neutron current vector. Then, the total number of neutrons leaking from the differential volume element, Fig. 4.7, is given by taking the normal component of this vector and integrating it over the differential volume element. That is

$$\text{Neutron leakage rate} = \int_{\Delta V} \vec{j}(\vec{r}) \cdot d\vec{A} \quad . \quad (4.18)$$

This vector integral expression can be reduced to a volume integration using the Divergence Theorem of vector algebra

$$\int_{\Delta V} \vec{j}(\vec{r}) \cdot d\vec{A} = \int_{\Delta V} \nabla \cdot \vec{j}(\vec{r}) dV \quad , \quad (4.19)$$

Here ∇ represents the del operator. Since Eq. (4.19) represents the total number of neutrons leaking from the volume element per second, then the number of neutrons leaking per unit volume per second is given by its integrant, thus

$$\text{Neutron leakage rate} = \nabla \cdot \underline{J}(\underline{r}) \quad . \quad (4.20)$$

The balance equation, Eq. (4.7), may now be written symbolically as

$$k_{\infty} \Sigma_a \phi(\underline{r}) = \Sigma_a \phi(\underline{r}) + \nabla \cdot \underline{J}(\underline{r}) \quad . \quad (4.21)$$

Although this equation is analytically correct for our simplified reactor model and thus far is free of any approximations, it is of little utility because it represents one equation in two functions: namely the neutron flux $\phi(\underline{r})$ and the neutron vector current $\underline{J}(\underline{r})$. A relationship between those two functions must be sought.

It is physically plausible to consider a neutron diffusion phenomena which describes the motion of neutrons from regions of high neutron density to regions of low neutron density; this process is similar to heat diffusion and mass diffusion. Indeed, the relationship is between the current quantity and the gradient of a density quantity; that is, the neutron current $\underline{J}(\underline{r})$ is proportional to the gradient of the neutron density, $n(\underline{r})$.

$$\underline{J}(\underline{r}) \propto -\nabla n(\underline{r}) \quad , \quad (4.22)$$

or, written in the form of a direct equality

$$\underline{J}(\underline{r}) = -\delta \nabla n(\underline{r}) \quad , \quad (4.23)$$

where δ is a constant. We use the definition of the neutron flux, $\phi(\underline{r}) = n(\underline{r})v$, into Eq. (4.23) and write

$$\underline{J}(\underline{r}) = -\delta \frac{\nabla}{v} \phi(\underline{r}) = -D \nabla \phi(\underline{r}) \quad . \quad (4.24)$$

Here, D is called the diffusion constant. Inserting Eq. (4.24) into Eq. (4.21) yields

$$k_{\infty} \Sigma_a \phi(\underline{r}) = \Sigma_a \phi(\underline{r}) + \nabla \cdot [-D \nabla \phi(\underline{r})] = \Sigma_a \phi(\underline{r}) - D \nabla^2 \phi(\underline{r}) \quad . \quad (4.25)$$

We may rewrite this equation in the more common form

$$\nabla^2 \phi(\underline{r}) + \left(\frac{k_{\infty} - 1}{L^2} \right) \phi(\underline{r}) = 0 \quad , \quad (4.26)$$

where

$$L^2 = D / \Sigma_a \quad . \quad (4.27)$$

This parameter L^2 is called the diffusion area and, pictorially, is proportional to the area swept out by a neutron from the time it appeared as a thermal neutron to the time it is absorbed.

Equation (4.26) represents the differential equation for the macroscopic flux in the one-speed description. Since the parameters k_{∞} and L^2 are constants we define

$$B_M^2 = \frac{k_{\infty} - 1}{L^2} , \quad (4.28)$$

where B_M^2 is called the material buckling. Note that it is fully described by the material composition of the homogeneous core since both parameters, k_{∞} and L^2 , depend only on the material.

In the following section we consider the solution to Eq. (4.26) and thus determine an additional condition relating the geometry of the cylindrical core to its material properties.

4.4 MACROSCOPIC FLUX

We summarize some of the salient points of our analysis thus far. The energy averaged neutron flux in cylindrical geometry of an unreflected homogeneous core satisfies a differential equation of the form

$$\nabla^2 \phi(\underline{r}) + B^2 \phi(\underline{r}) = 0 , \quad (4.29)$$

which, in cylindrical geometry and recognizing that for azimuthal symmetry the position vector \underline{r} is defined by the pair of coordinates (r, z) , is written as

$$\frac{1}{r} \frac{\partial}{\partial r} r \frac{\partial \phi}{\partial r} (r, z) + \frac{\partial^2 \phi}{\partial z^2} (r, z) + B^2 \phi(r, z) = 0 . \quad (4.30)$$

Finding a function $\phi(r, z)$ which satisfies this partial differential equation and the boundary conditions is now our objective. Fig. 4.7 shows the orientation of the coordinate system for the CANDU geometry.

We proceed to solve Eq. (4.30) based on two important, although very legitimate, assumptions for systems such as the CANDU reactor. We assume that under steady-state conditions the neutron flux in the r -direction is independent of the flux in the z -direction and hence propose a solution given by the product of two independent functions $\phi_r(r)$ and $\phi_z(z)$:

$$\phi(r, z) = \phi_r(r) \phi_z(z) . \quad (4.31)$$

Further, we assume that the neutron flux may be considered to be zero on the surface of the core. Both of these assumptions represent approximations but it is a remarkable fact that in spite of these assumptions and those embodied in the derivation of the neutron diffusion equation, Eq. (4.26), the resultant solution is a remarkably good approximation when applied to large homogeneous reactors of the CANDU type. Let us proceed with the solution.

We substitute the proposed solution form, Eq. (4.31) into Eq. (4.30) and, after some manipulation, obtain

$$\frac{1}{\phi_r(r)} \frac{d}{dr} r \frac{d\phi_r(r)}{dr} + \frac{1}{\phi_z(z)} \frac{d^2\phi_z(z)}{dz^2} + B^2 = 0 . \quad (4.32)$$

Since the first and second terms in this equation depend only on r and z respectively and together combine with a constant to add to zero, each of these functions must be equal to a constant. Hence, we write

$$\frac{1}{\phi_z(z)} \frac{d^2\phi_z(z)}{dz^2} = -\alpha^2 , \quad (4.33)$$

and

$$\frac{1}{\phi_r(r)} \frac{d}{dr} r \frac{d\phi_r(r)}{dr} = -\beta^2 , \quad (4.34)$$

where

$$B^2 = \alpha^2 + \beta^2 . \quad (4.35)$$

Thus, rather than solving one second order partial differential equation, we have two second order ordinary differential equations to solve; techniques for solving such ordinary equations are well known. We write immediately

$$\phi_z(z) = A_z \cos\left(\frac{\pi z}{L}\right) , \quad (4.36)$$

and

$$\phi_r(r) = A_r J_0\left(2.405 \frac{r}{R}\right) , \quad (4.37)$$

requiring that

$$\alpha^2 = \left(\frac{\pi}{H}\right)^2 , \quad (4.38)$$

and

$$\beta^2 = \left(\frac{2.405}{R}\right)^2 . \quad (4.39)$$

In writing down the above independent solutions, we have incorporated the zero-flux boundary condition referred to above and have required that only those solutions which are physically real - that is, finite everywhere - are taken into account. In addition, we have taken only the dominant terms which are applicable in a steady-state reactor. The function $J_0(2.405 r/R)$ is called an Ordinary Bessel function of Order Zero while $\cos(\pi z/L)$ is the trigonometric cosine function.

The macroscopic flux in the CANDU cylindrical reactor in our homogeneous core is thus given by

$$\phi(r,z) = A_0 J_0(2.405 \frac{r}{R}) \cos(\frac{\pi z}{H}) , \quad (4.40)$$

and the constant B^2 is

$$B^2 = (\frac{2.405}{R})^2 + (\frac{\pi}{H})^2 . \quad (4.41)$$

The radial flux, $\phi_r(r)$, and the axial flux, $\phi_z(z)$, are shown graphically in Fig. 4.8. Here we note that the neutron flux, and hence power densities peak in the center of the core and decrease toward the edges.

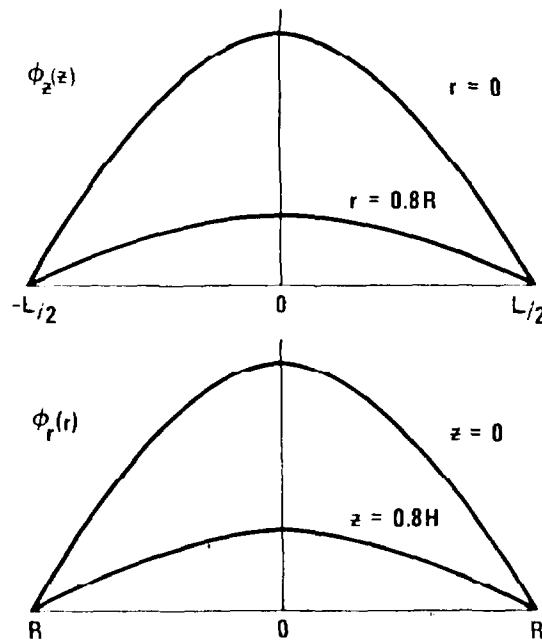


FIG. 4.8: Shape of the axial and radial neutron flux in a homogeneous cylindrical reactor at the center and near the edge in the axial and radial directions.

An important consideration is associated with the buckling parameter B^2 in Eq. (4.32). Here we have found that this term is expressed specifically in terms of the geometric properties of the core, that is, the length H and radius R , Eq. (4.41). For this reason, this is defined as the geometric buckling B_G^2

$$B_G^2 = \left(\frac{2.405}{R}\right)^2 + \left(\frac{\pi}{H}\right)^2, \quad (4.42)$$

to distinguish it from the material buckling B_M^2 , Eq. (4.28). Since both flux equations, Eq. (4.26) and Eq. (4.29) describe the neutron flux for a steady state critical reactor, the two bucklings must of necessity be the same. Hence the geometric properties are related to the material properties and we equate B_M^2 with B_G^2

$$\frac{k_\infty - 1}{L^2} = \left(\frac{2.405}{R}\right)^2 + \left(\frac{\pi}{H}\right)^2, \quad (4.43)$$

or, in a more common form

$$\frac{k_\infty}{1 + L^2 B_G^2} = 1. \quad (4.44)$$

Thus, to attain a steady-state critical reactor the materials composition must be so chosen and the reactor dimensions so specified that the parameters k_∞ , L^2 and B_G^2 satisfy Eq. (4.44).

4.5 HETEROGENEOUS CORE

In the above discussion we have assumed that the reactor core is homogeneous. Clearly, this is not the case in the CANDU core nor is it true for most other power reactors. Fuel, cladding, coolant, control rods and structural elements contribute to affect the neutron flux and cause it to deviate from the smooth representation as found in the preceding section and graphically displayed in Fig. 4.8. For example, consider the region on both sides of the pressure tube. To one side we have an insulating concentric air filled gap followed by the *calandria tube and the moderator*. Towards the other radial direction, there exists a repetitious lattice of D_2O coolant, zirconium fuel sheathing and nuclear fuel.

Insofar as the thermal neutron flux is concerned, it is possible to make some generalizations based on our previous discussion of neutron absorption and neutron slowing-down. In the fuel itself, we know that strong neutron absorption is taking place and hence the thermal neutron flux must be relatively low. On the other extreme, the thermal neutron flux in the moderator must be relatively high because it is in this region that neutron slowing down is particularly pronounced. Requiring continuity of the neutron flux and the neutron current we may readily sketch the neutron flux in this heterogeneous region, Fig. 4.9.

Consider now a fuel-element as a whole. Neutronic considerations similar to the analysis above suggest that a relative increase in the thermal neutron flux should occur at the end of each fuel bundle. In Fig. 4.10 we show the quantitative results from such a detailed microscopic flux calculation in both the radial

and axial direction in the vicinity of the end of a fuel bundle. We conclude that the detailed spatial thermal flux variations attributable to material heterogeneities must be superimposed on the smooth flux shape calculated for a homogeneous reactor core in the previous section, Fig. 4.8, for a more accurate description of the reactor core.

On a larger scale, the neutron flux is significantly affected by control rods and other flux modifying devices. These devices serve the important function of depressing the flux in the central region where - as was found in solving the diffusion equation for a homogeneous reactor, Fig. 4.8 - the neutron flux would normally be highest. These devices thus permit a more uniform burnup of fuel and provide for smaller temperature variations. The flux in an actual CANDU reactor in the axial direction is shown at two radial positions in Fig. 4.11. Note here, the three locations for the flux flattening and control rod devices.

As a final illustration we show a comparison between a calculated neutron flux and that obtained by direct measurement for an extreme case of non-symmetric flux distortion by a selective use of control rods, Fig. 4.12. The remarkable agreement between theory and experiment bears out the previous comment about the relevance and suitability of neutron diffusion analysis in CANDU reactors.

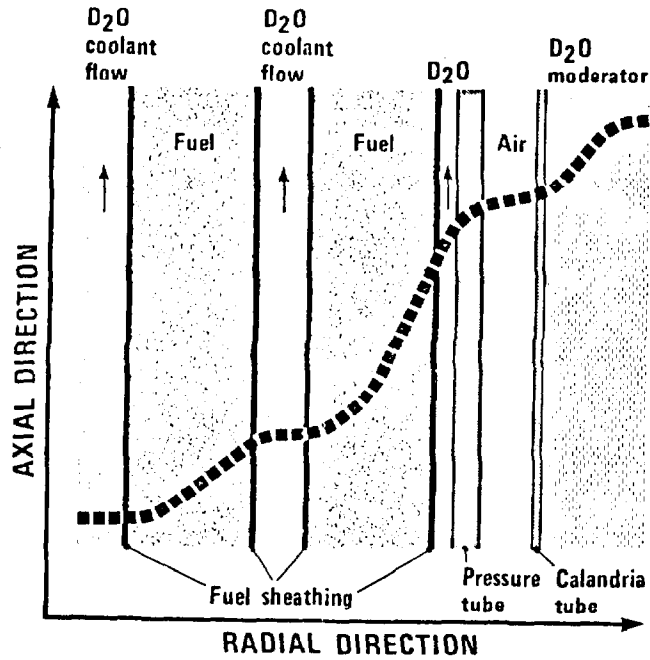


FIG. 4.9: Effect of material variations on the thermal neutron flux.

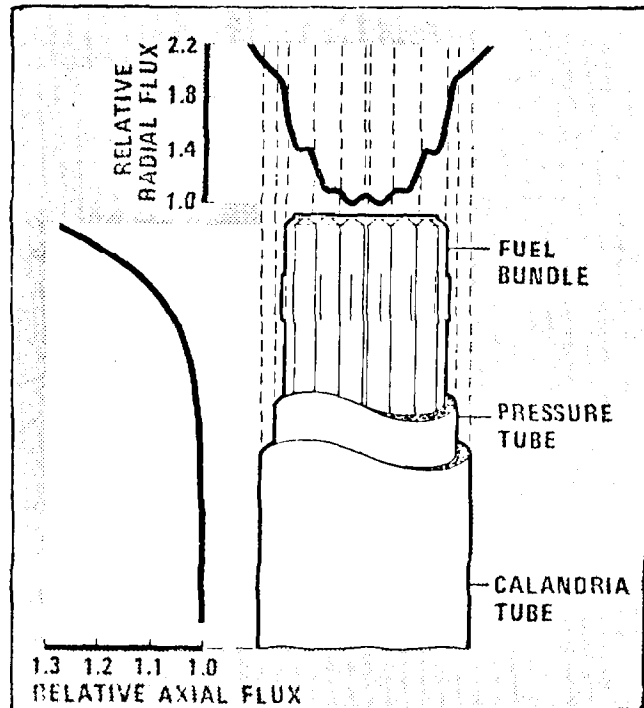


FIG. 4.10: Microscopic flux near the end of a fuel element.

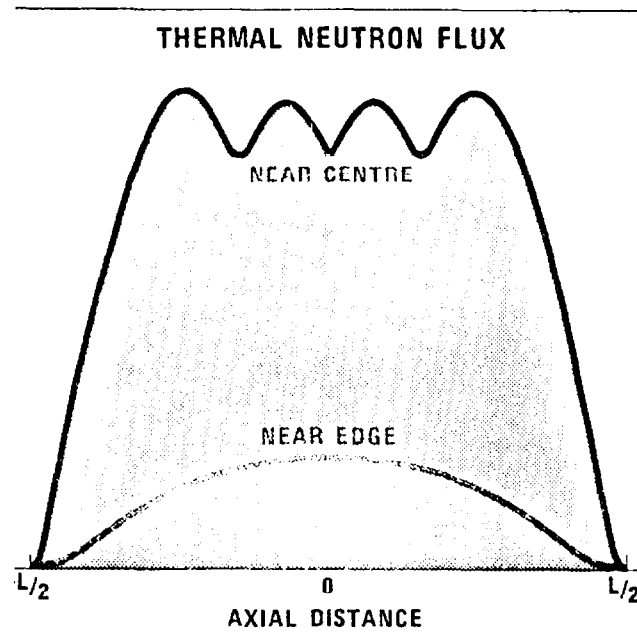


FIG. 4.11: Effect of reactor control devices on the macroscopic neutron flux.

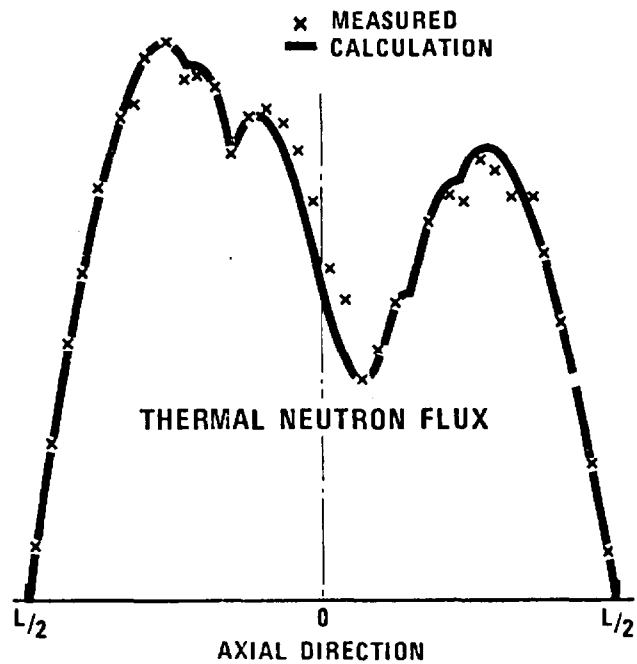


FIG. 4.12: Comparison between calculated and measured macroscopic neutron flux for the case of a severe flux distortion.

